ARTICLE NO. 79-0607R

Reduction of Wall Jet Trailing Edge Noise by Mean Flow Modification

M.C. Joshi*
Joint Institute for Advancement of Flight Sciences, Hampton, Va.

and

J.C. Yu†
NASA Langley Research Center, Hampton, Va.

The effect of mean flow modification on the trailing edge noise of a wall jet has been studied experimentally. Mean velocity profile at the nozzle exit was modified from the usual "top-hat" shape to Γ and L shaped profiles. The L shaped modification caused noise reduction around and above the peak frequency of the top-hat spectrum when compared on an equal thrust per exit area basis. Modification to a Γ shaped profile resulted in a shift of the spectrum to lower frequencies and a lower overall noise reduction. These modifications alter the development of the large-scale disturbances in the upper shear layer and trailing edge wake of the wall jet geometry.

Nomenclature

A = nozzle exit area, m^2
c_0 = ambient speed of sound, m/s
D = nozzle diameter, m
f = frequency, Hz
F = thrust, N
F_i = force per unit area exerted on the fluid by the solid boundaries in the x_i direction, N/m^2
H = nozzle height, m
l = screen mesh size
L = wall length, m
m = velocity exponent
p_D = acoustic pressure due to a dipole, N/m^2
p_Q = acoustic pressure due to a quadrupole, N/m^2
p_n = acoustic pressure at microphone n, N/m^2
$\overline{p^2}$ = mean square acoustic pressure, N^2/m^4
r = distance from the source to the observer, i.e., $|\vec{x}-\vec{y}|$, m
R_{mn} = cross-correlation between microphone m and microphone n, i.e., $\overline{p_m(t)p_n(t+\tau)}$, N^2/m^4
S = surface of integration
St = Strouhal number, i.e., fD/c_0
t = time, s
T_{ij} = stress tensor, N/m^2
U = local flow velocity, m/s
U_0 = mean flow velocity at nozzle exit, m/s
V = volume of integration
$\vec{x}$ = farfield vector
x_i, x_j = Cartesian coordinates and axes centered at trailing edge
x_0 = axial distance from nozzle exit, m
$\vec{y}$ = source vector
y_0 = normal distance from nozzle axis, m
γ^2_{mn} = coherence function between microphone m and microphone n
θ_1, θ_2 = angles described in Fig. 4, rad
ρ_{mn} = cross-correlation coefficient between microphone m and microphone n
τ = time delay, s

Superscripts and Subscripts

$(\bar{\ })$ = time average
$[\ ]$ = evaluation of the quantity within parentheses at retarded time
i or j = reference to direction x_i (or x_j), $i = 1,2$
m or n = reference to microphone m (or n), $m = 1,2,3,4$
TE = value at trailing edge station
max = peak value of a parameter

Presented as Paper 79-0607 at the AIAA 5th Aeroacoustics Conference, Seattle, Wash., March 12-14, 1979; submitted May 2, 1979; revision received Jan 28, 1980.

Index categories: Aeroacoustics; Noise; Jets, Wakes, and Viscid-Inviscid Flow Interactions.

*Post Doctoral Research Associate. Now Senior Engineer/Scientist, Acoustics Engineering, Douglas Aircraft Company, Long Beach, Calif. Member AIAA.

†Aerospace Technologist, Acoustics and Noise Reduction Division. Member AIAA.

Introduction

EXPERIMENTS such as the space-time correlations in the nearfield of a circular jet,[1] the response of a jet forced at the frequency of a disturbance that would grow naturally,[2] and the low Reynolds number flow visualization of shear layers[3] have all suggested the existence of ordered large-scale structures in turbulent jets. The significance of these organized large-scale structures in the production of jet noise has been studied recently by Sarohia and Massier.[4] Flow visualizations of the wall jet geometry[5,6] (a high velocity plane jet exhausting over a flat plate) have also revealed the presence of large-scale vortical structures in the free shear layer of the jet and in the trailing edge wake (TEW) downstream of the plate trailing edge (Fig. 1). This structure of the wall jet flowfield bears a good resemblance to that observed in plane mixing layers by Brown and Roshko.[3] The disturbance seems to grow as it moves away from the nozzle exit. While the importance of large-scale structures in jet noise production is still under investigation,[4] an experimental study by Yu and Tam[7] has shown the dominant part of the wall jet trailing edge noise to be due to the interaction of the large-scale quasi-orderly disturbance covecting in the free shear layer with the plate trailing edge. This interaction produces a coherent dipole-type radiation in the direction normal to the wall plane. It also generates large-scale vortical motion in the TEW, resulting in intense turbulent mixing downstream of the trailing edge.

The recognition of the existence of such large-scale disturbance and its relation to the radiated noise suggests a new approach for jet noise and wall jet trailing edge noise

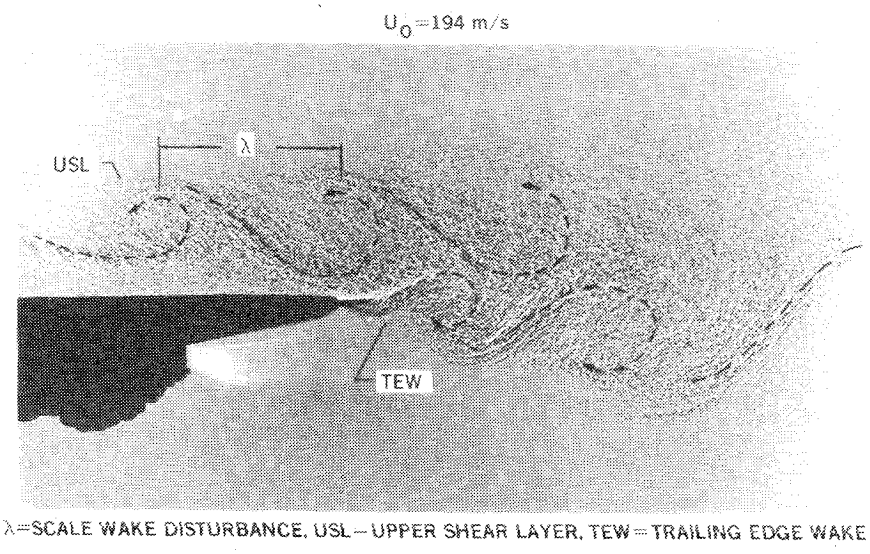

Fig. 1 Spark shadowgraph showing flowfield near wall jet trailing edge.

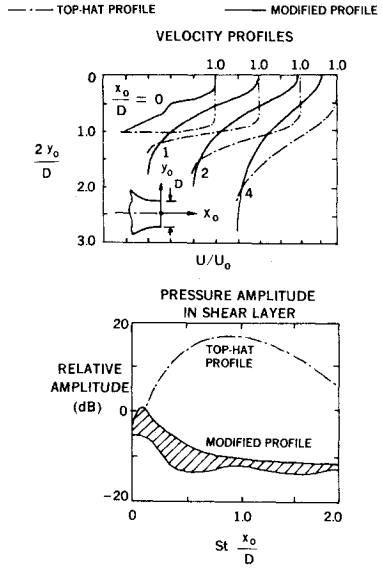

Fig. 2 Suppression of spatial waves in shear layers (from Ref. 9).

reduction: suppress the growth of the disturbance. One such avenue for jet noise reduction has been recognized by Arndt, Fuchs, and Michel[8] in a study of jet noise suppressors that attempt the breaking up of the coherent structures by such means as quin-axial tubes, corrugated nozzles, mesh-covered nozzles, and screen tubes. The approach used in the present wall jet noise reduction study, on the other hand, utilizes the knowledge of the growth of shear layers. The initial development of large-scale disturbances is governed by the hydrodynamic stability theory for shear flows where the main flow distribution plays an important role. A shear layer having a velocity profile with moderate velocity gradients does not support a wave disturbance propagating downstream. It has been shown experimentally by Chan and Templin[9] that a disturbance wave in a turbulent circular jet is rapidly amplified by a top-hat type or uniform velocity profile. The wave reaches its maximum amplitude at $Stx/D=0.8$ (St = Strouhal number based on diameter D) and decays farther downstream (Fig. 2). When the velocity profile at the nozzle exit is modified to a bell-shaped profile, the disturbance is not amplified; instead, it decays rapidly downstream of the nozzle exit. By modeling the source structure as a traveling instability wave that grows and decays in amplitude and has a random component in its phase velocity, Ffowcs Williams and Kempton[10] were able to show that the rate of change from growth to decay determines the magnitude of the radiated sound while the randomness in the phase velocity determines its spectrum. A favorable change in the growth and decay process of the disturbance wave in the free shear layer of a jet with modified velocity profile can then be expected to result in reduced noise production. It is the objective of the present study to establish experimentally the concept of wall jet trailing edge noise reduction by altering the development of the large-scale disturbance in the shear layer through mean flow modification.

The wall jet geometry is of practical interest because of its similarity to upper surface blowing (USB) high lift systems such as the YC-14 and the QCSEE-OTW configurations. In these high lift systems, the trailing edge noise has been known to be a major contributor to community noise. Recent measurements[11] have shown that the QCSEE-OTW configuration's takeoff noise level exceeds the 95 EPNdB noise goal by at least 3 EPNdB. A study of the means of alleviating the trailing edge noise is therefore of practical importance. It should be noted that the flow similarity between a wall jet and a USB lift system can be expected for moderate flap angles. (The QCSEE-OTW configuration at takeoff flap angle setting produces a flow turning angle of only 30 deg.) For large flap angles, the effects of flap surface curvature must be considered.

Experimental Arrangement

The model wall jet used in the present study was the same as those used in the investigation by Yu and Tam.[7] The nozzle exit was rectangular with dimensions 15 by 1.5 cm. The stilling chamber/nozzle exit area ratio was 22.5. The flat plate used with the nozzle had a chord length L 8.5 times the nozzle height H and a span of 61 cm. The trailing edge of the plate was machined to a knife edge. Mean flow modification was achieved by means of three 80 mesh wire screens inserted within the upper or lower half of the nozzle height. The splitter plate that held the screens in place was 0.16 cm thick and was also sharpened to a thin edge at its nozzle exit. For the 80 mesh screen ($l=1/80$ in.) the distance to the nozzle exit is then greater than 200 l, which is considered adequate for the screen-generated turbulence to decay to a low value at the nozzle exit. Two modifications of the reference top-hat or uniform velocity profile were obtained: the Γ profile with screens in the lower half of the nozzle and the L profile with screens in the upper half. The variations, as is obvious from Fig. 3, are named after the shape of the profile. In full sized engines, such profiles should, of course, be obtained by appropriate ducting of the fan flow.

The thrust of the nozzle or wall jet was measured by means of a large thick plate pivoted along its midlength on smooth bearings. Impingement of the jet on one-half of the plate

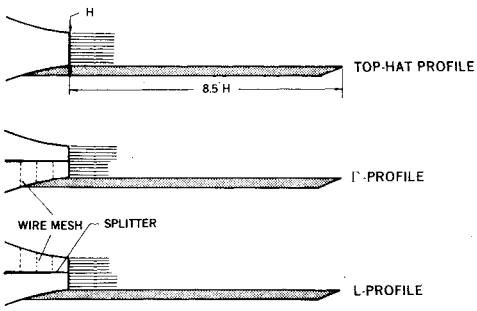

Fig. 3 Mean velocity profiles investigated.

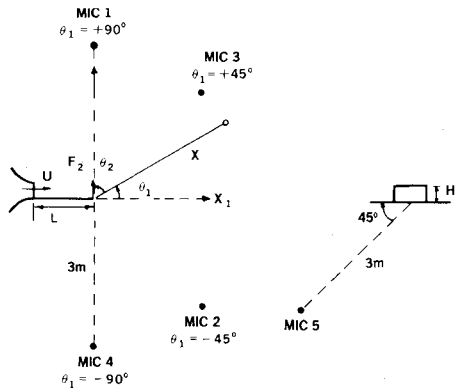

Fig. 4 Schematic showing microphone arrangement and coordinate system.

exerted a force on the load cell on which the other half of the plate was resting. This force was a measure of the thrust of the impinging jet. Velocity profiles in the jet or wall jet were obtained by traversing a total pressure tube along the height of the nozzle. This was done in the midspan plane at several stations along the jet by means of a *DISA* traversing rig. The rig had a linear resolution of 0.1 mm, and the traverse was done at a slow rate to allow adequate averaging. Flowfield visualization was done using spark shadowgraphy.

The farfield noise was measured by means of Bruel & Kjaer 1.27 cm (0.5 in.) freefield microphones. Four microphones were placed in the flyover plane (Fig. 4) at a nominal distance of 3 m from the plate trailing edge. Microphones above the plate at $\theta_1 = +90$ and $+45$ deg will be referred to as microphones 1 and 3, respectively, and those below the plate at $\theta_1 = -45$ and -90 deg as microphones 2 and 4. A fifth microphone was used to measure the sideline noise as shown in Fig. 4. All of the measurements were done in an anechoic flow facility at NASA Langley Research Center. Farfield noise data from all of the microphones were simultaneously recorded in the FM mode on an Ampex tape recorder for later analysis using a time series analysis program and/or a Spectral Dynamics SD-360 Signal Processor. The recorder response was flat up to 20 kHz.

Evaluation of Noise Reduction

In order to establish the effectiveness of a noise reduction concept, a basis of evaluation must be selected. Equal total thrust is the most common basis of comparison. In the present study, however, thrust per unit exit area was chosen as the basis for the following reason: the objective of the study is to establish the effect of mean velocity profile modification on the wall jet noise, and the screen insert is the simplest arrangement to produce profile shaping. However, the finite sectional area of the insert caused a blockage of about 15% of the total exit area. It is therefore assumed that the modified nozzle is a scaled-down version of the one that should be the equivalent of the unmodified nozzle. This area factor is accounted for if a comparison is made on a constant thrust per unit area basis. This basis of comparison was also used in Ref. 8. If no allowance is made for the area blockage and if the comparison of noise reduction is based upon constant total thrust, the noise reduction would be about 2 dB lower, assuming a U^6 dependence for farfield noise.

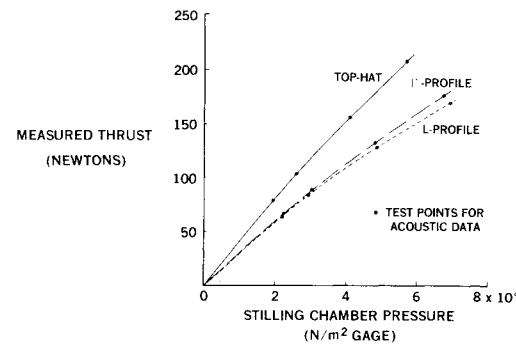

Fig. 5 Variation of thrust with total pressure.

Another practical aspect of the performance basis is the base drag due to the splitter plate. From the static pressure measurements of Blake[12] on struts with blunt and rounded trailing edges, it was estimated that the maximum base drag of the present splitter plate is about 4% of the total thrust. This would introduce a discrepancy of only 0.5 dB in the noise comparison, again assuming a U^6 dependence of farfield noise.

Flowfield Data

Thrust measurements were made for several values of the stilling chamber total pressure for the top-hat, Γ, and L profile configurations in order to be able to select pressure values that give equal thrust per unit exit area for the three profiles. These measurements are plotted in Fig. 5. The screen insert for the Γ profile causes approximately 27% thrust loss over the entire total pressure range. For the Γ profile, the thrust loss is slightly higher. This is because the inserts used to produce the Γ and L profiles were not exactly identical, the area blockage due to the latter being slightly higher than that due to the former. Four sets of operating points corresponding to thrust per unit exit area $F/A = 34{,}475$, 45,967, 68,950, and 91,931 N/m^2 were chosen for acoustic tests and are represented by solid symbols in the figure.

The effect of mean velocity profile modification on the wall jet flowfield was examined by means of spark shadowgraphy and pitot pressure surveys. The shadowgraphs for the top-hat profile showed two major regions of large-scale activity—the upper shear layer (USL) downstream of the nozzle exit and the trailing edge wake (TEW) aft of the trailing edge. Figures 6 and 7 show the effects of mean flow modification on the large-scale disturbances in the USL and the TEW, respectively, for a thrust setting of $F/A = 68{,}950$ N/m^2. This condition corresponds to a Reynolds number of 2×10^6 based upon the plate length and mean jet exit velocity. As observed in Fig. 6a for the top-hat profile, the large-scale structure in the USL has counterclockwise vorticity and grows in size as it moves downstream. Modification of the profile to a Γ shaped profile causes the effective length of the upper potential core to become almost half that of the top-hat profile (Fig. 6b). The large-scale structures in the USL still exist, but their extent across the jet is reduced. For the L profile (Fig. 6c) large-scale activity in the USL is not as clearly defined as for the top-hat and Γ shaped profiles. The structure in the TEW shown in Fig. 7a for the top-hat profile has the shape of a shed vortex with clockwise vorticity. It grows considerably within a short distance from the trailing edge. The large-scale structure in the TEW of the Γ profile configuration (Fig. 7b) is much weaker in comparison to that for the top-hat profile. For the L profile (Fig. 7c) no large-scale disturbance is ob-

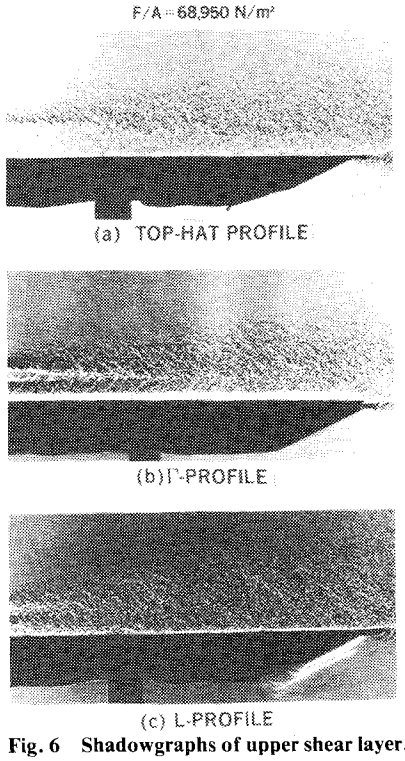

Fig. 6 Shadowgraphs of upper shear layer.

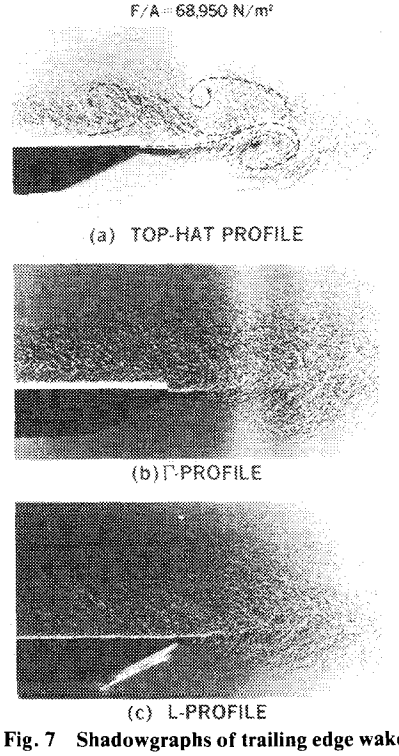

Fig. 7 Shadowgraphs of trailing edge wake.

served in the TEW except for a rollup immediately downstream of the plate. These effects were also seen at other thrust settings. In summary, Figs. 6 and 7 show that mean velocity profile modification alters the large-scale disturbance activity both in the USL and in the TEW. While the L profile considerably suppresses the large-scale structures in both the USL and the TEW, the major influence of the Γ profile is in the TEW.

The total pressure profiles measured using the pitot tube were converted to mean velocity profiles by means of gas dynamic equations. These profiles for several stations along

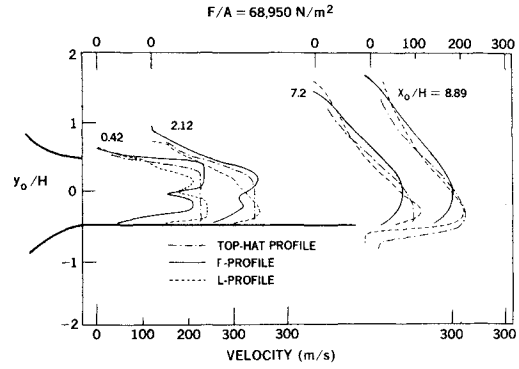

Fig. 8 Measured velocity profiles.

the flow are plotted in Fig. 8 for the top-hat, Γ, and L profile configurations operating at $F/A = 68{,}950$ N/m^2. They show the differences in the development of the flowfield for the three profile shapes. The set of profiles at $x_0/H = 0.42$ indicates that the screen inserts are fairly successful in modifying the mean velocity profile to the desired shape except for the dip due to the splitter wake. Furthermore, the inserts for the Γ and L profiles produce nearly identical (but on the opposite side of the jet centerline) modifications of the top-hat profile. At this station the velocity gradient in the free shear layer is moderately low for the L profile compared to those for the Γ shaped and top-hat profiles. This smoothing of the mean velocity distribution apparently affects the growth of the large-scale disturbances, as is obvious in the shadowgraphs of Fig. 6. Comparisons of profiles at locations further downstream indicate considerable difference in the growth of the wall jet flow. Near the trailing edge, $x_0/H = 8.89$, the L profile has a velocity distribution that is only slightly different from the top-hat profile, but the Γ profile has a slightly higher velocity gradient in the free shear layer and a thicker boundary layer that causes a lower velocity gradient near the wall. Its effect is reflected in the shadowgraph (Fig. 7b) as a weakened large-scale structure in the TEW of the Γ profile configuration. Since turbulence production depends upon the mean velocity gradient and since considerable differences exist in the velocity profiles near the trailing edge, the TEW characteristics may be expected to be different for the three profile shapes.

Farfield Noise Data

The effect of mean velocity profile modification on the trailing edge noise production can be seen by comparing the farfield noise spectra in several directions of radiation for the three profile shapes. Figures 9 and 10 show one-third octave band sound pressure level comparisons for microphone 4 ($\theta_1 = -90$ deg) and microphone 2 ($\theta_1 = -45$ deg), respectively, the thrust setting being $F/A = 68{,}950$ N/m^2. It can be seen that the modified profiles produce reduced noise levels at frequencies around and above the spectral peak of the top-hat profile. The Γ profile, however, increased the levels at lower frequencies. Thus, the L profile provided a better overall noise reduction, while the Γ profile generally caused a redistribution of acoustic energy to lower frequencies. Directionally, maximum noise reduction in the flyover plane was observed at microphone 2 ($\theta_1 = -45$ deg). This can be seen in Fig. 10 to be on the order of 6 dB in one-third octave bands for frequencies near and greater than the peak frequency of the unmodified top-hat profile. The overall (OASPL) noise reduction was 1.8 dB for the Γ profile and 3.6 dB for the L profile. At the position of microphone 3 ($\theta_1 = +45$ deg), the effects of mean flow modification were of lower magnitude. The general trends discussed above were observed for all thrust values, but the noise reduction was, in general, greater at higher thrust settings. The effect of profile

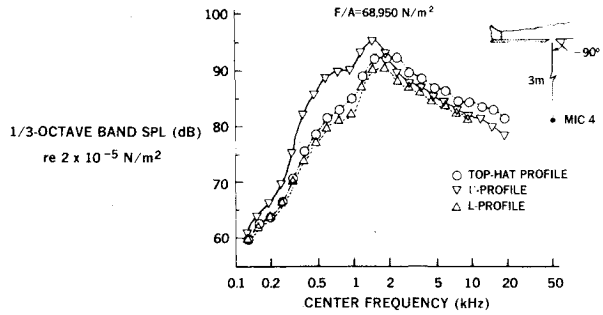

Fig. 9 Farfield noise spectrum (microphone 4).

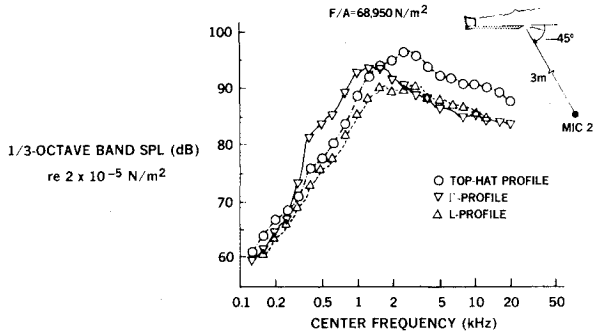

Fig. 10 Farfield noise spectrum (microphone 2).

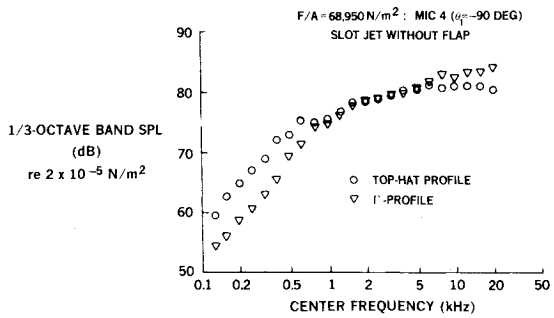

Fig. 11 Effects of mean flow modification on jet noise.

modification on the sideline noise radiation (microphone 5) was not much different from that observed in the flyover plane. The reduced levels in all directions are an indication that the reduction is in the total power produced as opposed to a redistribution in space of the radiated power. It should be noted that the acoustic effects of the mean velocity profile modifications for the wall jet geometry are different from their effects on free jets. In a study of the effect of mean profile modification on jet noise, Crouch, et al.,[13] observed that the inverted velocity profile caused a reduction in low frequency components and an increase in high frequency components. The Γ profile free jet, which is a two-dimensional equivalent of the axisymmetric inverted velocity profile jet, showed similar spectral effects (see Fig. 11).

An interesting characteristic of the radiation field for the wall jet geometry is shown in Fig. 12, which plots the peak levels in one-third octave spectra vs the maximum velocity ($U_{TE_{\max}}$) near the trailing edge ($x_0/H = 8.89$). For all three profile shapes, the SPL is proportional to about the sixth power of $U_{TE_{\max}}$ for microphone 4 ($\theta_1 = -90$ deg) and about the eighth power for the microphone 2 ($\theta_1 = -45$ deg) location. The velocity exponents are represented by m in the figure. Furthermore, as shown in Fig. 13, the acoustic spectra for different velocities at microphone 2 collapse fairly well when the SPL is normalized by the eighth power of $U_{TE_{\max}}$ and the frequency by $U_{TE_{\max}}$. The spectra at microphone 4 collapse when the SPL is normalized by the sixth power of

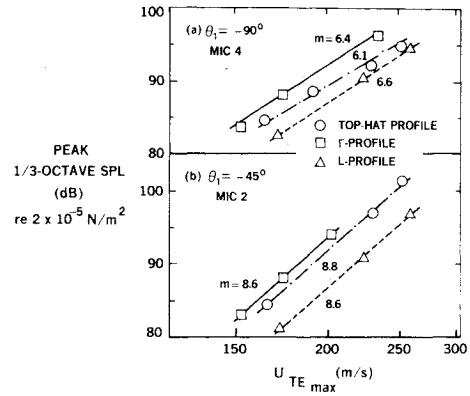

Fig. 12 Velocity power laws for microphone 2 and microphone 4.

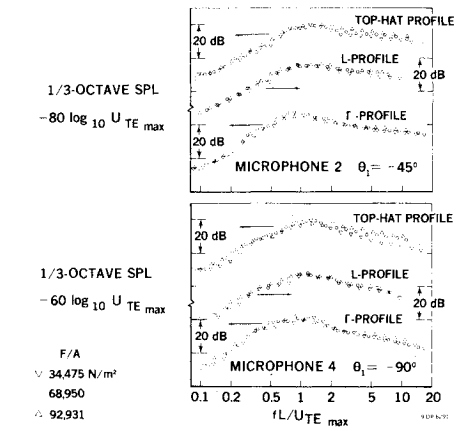

Fig. 13 Normalized farfield spectra.

$U_{TE_{\max}}$. Brown, et al.,[14] in a study of a model upper surface blowing lift system, found the velocity dependence to increase from a value of nearly 5 at the $\theta_1 = -90$ deg position to about 7.5 as the $\theta_1 = -45$ deg direction was approached. Such a variation in the velocity exponent suggests the possibility of preferential directional radiation from certain regions of the flowfield. The U^8 dependence of a quadrupole-generated field and the U^6 dependence of a dipole-generated field can be used to identify significant contributions to the wall jet acoustic field in the $\theta_1 = -45$ deg direction from the TEW and the dominance of a dipole-type field in the $\theta_1 = \pm 90$ deg directions. The study by Yu and Tam[7] clearly identified the acoustic field to be in phase opposition across the plate in $\theta_1 = \pm 90$ deg directions for the unmodified top-hat wall jet geometry. Furthermore, it showed that the acoustic field was due to the interaction between the trailing edge and the large-scale disturbance convecting in the upper shear layer. Becker's investigation[15] of the acoustic field in $\theta_1 = \pm 45$ deg directions for a smaller wall jet model showed the trailing edge wake to be the dominant noise contributor in the $\theta_1 = -45$ deg direction. However, as pointed out in Ref. 7, due to the proximity of the shear layer to the wall, the passage of the USL large-scale disturbance past the trailing edge forces the TEW into large-scale oscillations. This causes the USL to be the most important flow region for the wall jet geometry. Besides radiating a dipole-type field by its interaction with the trailing edge, it produces a large-scale disturbance in the wake, which, with the high turbulent mixing, becomes an efficient quadrupole radiator.

Cross-correlations among microphones in the flyover plane showed the broadband sound radiation to be in phase opposition across the wall plane for all the mean velocity profile shapes. In other words, the cross-correlation had a negative peak if the microphones were on opposite sides of the wall plane and a positive peak for microphones on the same side.

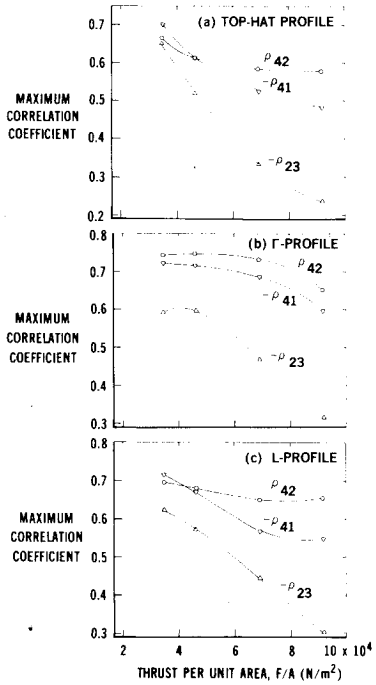

Fig. 14 Variation of normalized correlations with thrust.

Furthermore, the time delay at which the correlation peaked suggested that the source of the antiphase sound radiation is at the trailing edge. Another interesting characteristic of the wall jet radiation field can be observed in Fig. 14, which shows plots of the maximum normalized correlation against measured thrust per unit exit area for the microphone pairs: microphone 4 × mircophone 1, microphone 4 × microphone 2, and microphone 2 × microphone 3. These correlations are seen to decrease in value with increasing thrust, indicating a loss in coherence. Among the three pairs of correlations, $\rho_{23\max}$ decreases most while $\rho_{42\max}$ decreases least. At higher thrust setting, $\rho_{42\max}$ has a value greater than $\rho_{41\max}$ and considerably greater than $\rho_{23\max}$. This is observed for all three profiles and suggests that at high thrust settings the wall jet geometry radiates a sound field that is more coherent in the 4-2 direction, i.e., below the wall plane.

It is pertinent to point out that the amount of noise reduction obtained through mean flow modification is not simply related to the maximum velocity at the trailing edge. The local maximum velocity at the trailing edge for the Γ profile is less than that for the top-hat profile (for the same F/A), but the L profile configuration has values greater than, or equal to, the top-hat value. The nearly identical velocity power laws for the three profile shapes, both at the $\theta_f = -45$ and -90 deg locations, and the similarity of the joint statistics of the farfield microphones imply no change in the noise production mechanisms due to mean flow modification. Greater noise reductions in the $\theta_f = -45$ deg direction compared to other directions in the flyover plane suggest that mean flow profile modification causes considerable change in the trailing edge wake noise production. This possibility is, of course, supported by the shadowgraphic observations, which showed the large vortical structure in the wake of the top-hat configuration to weaken when the mean flow was modified to a Γ shaped profile and almost disappear when modified to an L shaped profile. The suppression of the growth of large-scale disturbance in the USL by mean flow modification reduces its interaction with the trailing edge and is responsible for the noise reduction observed in $\theta_f = \pm 90$ deg directions.

The maximum coherence values for pairs of microphones in the flyover plane are plotted vs the thrust setting in Fig. 15 for the three mean flow profiles. It can be noticed that the coherence decreases when the top-hat profile is modified to an

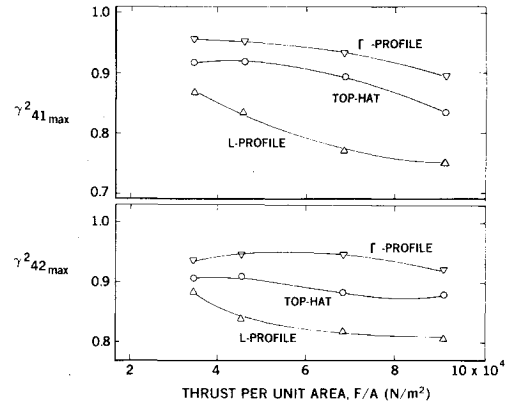

Fig. 15 Variation of coherence functions with thrust.

L shaped profile, but increases slightly when modified to a Γ shaped profile. Based upon these joint statistics, shadowgraphic observations, and measured velocity profiles, it can be said that the L profile is effective in suppressing the growth of the large-scale disturbance in the shear layer at the nozzle exit. Since the TEW is coupled to the USL, the suppression of the large-scale disturbance in the USL also reduces the large-scale activity in the TEW. This causes the sound radiators to be less coherent. The Γ shaped modification, on the other hand, increases the gradient in the USL, which may aid the growth of the disturbance and make the large-scale structures more coherent. However, the lower mean velocity on the wall side results in a broad, smooth velocity distribution near the trailing edge and this in turn weakens the large-scale activity in the TEW. The direct effect of the L shaped modification on the large-scale disturbance in the USL may be the cause of its greater noise benefit.

As mentioned before, wall curvature can have some effect on the development of the mean flowfield and, consequently, on the noise generated by the wall jet. It is expected that the Γ profile will be more susceptible to separation from a curved surface than the L profile. In the QCSEE-OTW study, the nearly L shaped mean flow remained attached to the curved flap surface even for a flap angle of 75 deg, corresponding to approach. The possibility of flow separation for the Γ profile and the acoustic effects of forward flight for both L and Γ profiles must be investigated.

Analytical Considerations

Since experimental observations have shown that the wall jet acoustic field consists of a dipole-type radiation that is antiphase across the wall plane and a quadrupole-type radiation with preferred radiation in the $\theta_f = -45$ deg direction, we can model the wall jet geometry by means of a dipole and a lateral quadrupole, both in the proximity of the wall trailing edge, to evaluate the contribution to the farfield of the individual sources in terms of the correlation between the farfield microphones. This model can be used to determine the effect of mean flow modification on the constituent sources. It is realized that such modest modeling could be unrealistic, but in the absence of any inflow measurements (except mean velocity), some assumptions regarding the source field must be made. The validity of these assumptions will, of course, be determined by the final results and the extent of their agreement with the experiments.

With the coordinate system of Fig. 4 and standard notation, we know that the pressure field due to a dipole and quadrupole is given respectively by

$$p_D = \frac{1}{4\pi}\frac{\partial}{\partial x_i}\int_S \frac{[F_i]}{r}\,dS(\vec{y}) \tag{1a}$$

and

$$p_Q = \frac{1}{4\pi}\frac{\partial^2}{\partial x_i \partial x_j}\int_V \frac{[T_{ij}]}{r}\,dV(\vec{y}) \tag{1b}$$

If the sources are compact, then at a farfield observation point $\vec{x}$

$$p_D = \frac{\cos\theta_2}{4\pi c_0 x}\left[\frac{\partial F_2}{\partial t}\right] \tag{2a}$$

and

$$p_Q = \frac{\cos\theta_1\cos\theta_2}{4\pi x c_0^2}\left[\frac{\partial^2 T_{12}}{\partial t^2}\right] \tag{2b}$$

The total radiated pressure field

$$p = p_D + p_Q = \frac{\cos\theta_2}{4\pi c_0 x}\left\{\left[\frac{\partial F_2}{\partial t}\right] + \frac{\cos\theta_1}{c_0}\left[\frac{\partial^2 T_{12}}{\partial t^2}\right]\right\} \tag{3}$$

For the microphone 1 position $\theta_1 = \pi/2$ and $\theta_2 = 0$

$$p_1 = \frac{1}{4\pi c_0 x}\left[\frac{\partial F_2}{\partial t}\right] \tag{4a}$$

For the microphone 4 position $\theta_1 = -\pi/2$ and $\theta_2 = \pi$

$$p_4 = \frac{-1}{4\pi c_0 x}\left[\frac{\partial F_2}{\partial t}\right] \tag{4b}$$

the cross-correlation of the pressures at microphones 4 and 1 can then be written as

$$\overline{p_4(t)p_1(t+\tau)} = -\frac{1}{(4\pi c_0 x)^2}\left[\frac{\partial F_2(t)}{\partial t}\frac{\partial F_2(t+\tau)}{\partial t}\right] = \frac{1}{(4\pi c_0 x)^2}\frac{\partial^2}{\partial \tau^2}\overline{[F_2(t)F_2(t+\tau)]} \tag{5}$$

Similarly, for microphone 3 position $\theta_i = \pi/4 = \theta_2$

$$p_3 = \frac{1}{\sqrt{2}4\pi c_0 x}\left\{\left[\frac{\partial F_2}{\partial t}\right] + \frac{1}{\sqrt{2}c_0}\left[\frac{\partial^2 T_{12}}{\partial t^2}\right]\right\} \tag{6a}$$

and for microphone 2 positions $\theta_1 = -\pi/4, \theta_2 = 3\pi/4$

$$p_2 = \frac{-1}{\sqrt{2}4\pi c_0 x}\left\{\left[\frac{\partial F_2}{\partial t}\right] + \frac{1}{\sqrt{2}c_0}\left[\frac{\partial^2 T_{12}}{\partial t^2}\right]\right\} \tag{6b}$$

Assuming the two sources to be uncorrelated

$$\overline{p_2(t)p_3(t+\tau)} = \frac{1}{2(4\pi c_0 x)^2}\left[\frac{\partial^2}{\partial \tau^2}\overline{F_2(t)F_2(t+\tau)}\right] - \frac{1}{4c_0^2(4\pi c_0 x)^2}\left[\frac{\partial^4}{\partial \tau^4}\overline{T_{12}(t)T_{12}(t+\tau)}\right] \tag{7}$$

The individual contributions of the sources can now be evaluated. It follows from Eqs. (2a) and (5) that

$$\overline{p_D(t)p_D(t+\tau)} = -\cos^2\theta_2\,\overline{p_4(t)p_1(t+\tau)} \tag{8a}$$

The sound field due to the dipole is then given by

$$\overline{p_D^2} = -\cos^2\theta_2\,[R_{41}]_{\tau=0} \tag{8b}$$

Similarly, it follows from Eqs. (2b,5, and 7) that

$$\overline{p_Q(t)p_Q(t+\tau)} = -\sin^2 2\theta_2\left\{\overline{p_2(t)p_3(t+\tau)} - \frac{1}{2}\overline{p_4(t)p_1(t+\tau)}\right\} \tag{9a}$$

The quadrupole sound field is then given by

$$\overline{p_Q^2} = -\sin^2 2\theta_2\left\{[R_{23}]_{\tau=0} - \frac{1}{2}[R_{41}]_{\tau=0}\right\} \tag{9b}$$

The combined sound field due to the dipole and the quadrupole can be obtained from

$$\overline{p^2} = \overline{p_D^2} + \overline{p_Q^2} \tag{10}$$

It should be noted that Eqs. (8b) and (9b) have the directivities assumed for the respective sources. The assumed sources produce a resultant field that is in phase opposition across the wall plane. While this source representation is by no means a unique representation of the measured farfield, perhaps it is the simplest. Reconstruction of the data with the least singular distribution of uncorrelated sources to overcome the issue of uniqueness has been common practice in acoustics (see, for example, Mani, et al.[16]).

The measured cross-correlations among the farfield microphones were used in Eqs. (8b,9b), and (10) to estimate the individual source contribution in each of the three mean flow profile configurations. The change in source contribution due to a change in the mean flow profile was estimated by using the value for the top-hat profile as reference. These values are tabulated in Table 1. We note from columns 8 and 12 of the table that modification of the top-hat mean flow profile to an L shaped profile should produce greater overall noise reductions than a Γ shaped modification. The noise reduction should furthermore be higher at the microphone 2 location than at the microphone 4 location. It also shows large reductions in the quadrupole contribution due to mean flow modification (column 6) and comparatively smaller reductions or even an increase in the dipole contribution (column 4). The general trend of these

Table 1 Dipole and quadrupole sound calculations using farfield cross-correlation measurements

		Microphone 2						Microphone 4			
F/A, N/m^2	Configuration	$\overline{p_D^2}$, N^2/m^4	Δp_D, dB	$\overline{p_Q^2}$, N^2/m^4	Δp_Q, dB	$\overline{p^2}$, N^2/m^4	Δp, dB	$\overline{p_D^2}$, N^2/m^4	Δp_D, dB	$\overline{p_D^2}$, N^2/m^4	Δp, dB
91931	TH	2.376	0	3.745	0	6.121	0	4.752	0	0	0
	Γ	2.013	−0.72	1.626	−3.62	3.639	−2.26	4.025	−0.72	0	−0.72
	L	2.978	0.98	0.417	−9.53	3.395	−2.56	5.955	0.98	0	0.98
45967	TH	0.353	0	0.393	0	0.746	0	0.705	0	0	0
	Γ	0.422	0.78	0.390	−0.04	0.811	0.37	0.843	0.78	0	0.78
	L	0.267	−1.07	0.062	−7.99	0.338	−3.4	0.552	−1.07	0	−1.07
34475	TH	0.172	0	0.171	0	0.344	0	0.344	0	0	0
	Γ	0.164	−0.2	0.078	−3.43	0.242	−1.52	0.329	−0.2	0	−0.2
	L	0.175	0.07	0.021	−9.18	0.196	−2.44	0.350	0.07	0	0.07

estimates is in agreement with experimental observations reported in the previous section.

Summary

The effect of mean flow velocity profile modification on the noise reduction of a wall jet (a high velocity jet exhausting over a flat plate) has been studied experimentally with application to high lift systems in mind. The usual top-hat profile was modified to Γ shaped and L shaped profiles. The L shaped modification produced a maximum noise reduction of 6 dB in one-third octave bands around and above the peak frequency of the top-hat spectrum when compared on an equal thrust per exit area basis. The Γ profile, in general, resulted in a shift of the spectrum to lower frequencies and, therefore, lower overall noise reduction. Maximum noise reduction was observed in the $\theta_1 = -45$ deg direction below the plate. The noise benefit was higher at higher thrust settings.

It is believed that mean flow modification causes a change in the growth of the large-scale disturbance in the USL, which reduces its interaction with the trailing edge and results in a consequent reduction in the dipole-type noise radiation in the $\theta_1 = \pm 90$ deg directions. The coupling between the USL and the TEW and the dependence of turbulence production in the wake upon the mean velocity gradients near the trailing edge cause the large-scale activity in the TEW to weaken, resulting in a reduction of the quadrupole-type noise radiation in directions below the plate.

References

[1] Mollo-Christensen, E., "Jet Noise and Shear Flow Instability Seen from an Experimenter's Viewpoint," *Journal of Applied Mechanics*, Vol. 34, March 1967, pp. 1-7.

[2] Crow, S.C. and Champagne, F.H., "Orderly Structure in Jet Turbulence," *Journal of Fluid Mechanics*, Vol. 48, Part 3, 1971, pp. 547-591.

[3] Brown, G.L. and Roshko, A., "On Density Effects and Large-Scale Structures in Turbulent Mixing Layers," *Journal of Fluid Mechanics*, Vol. 64, 1974, pp. 775-816.

[4] Sarohia, V. and Massier, P.E., "Experimental Results of Large-Scale Structures in Jet Flows and Their Relation to Jet Noise Production," *AIAA Journal*, Vol. 16, Aug. 1978, pp. 831-835.

[5] Tam, C.K.W. and Yu, J.C., "Trailing Edge Noise," *Progress in Astronautics and Aeronautics*, Vol. 45, 1976, pp. 259-280.

[6] Patterson, G.T., Joshi, M.C., and Maus, J.R., "Experimental Investigation of the Aeroacoustic Characteristics of Model Slot Nozzles with Straight Flaps," *Progress in Astronautics and Aeronautics*, Vol. 45, 1976, pp. 41-57.

[7] Yu, J.C. and Tam, C.K.W., "An Experimental Investigation of the Trailing Edge Noise Mechanism," AIAA Paper 77-1291 presented at the AIAA 4th Aeroacoustics Conference, Atlanta, Ga., 1977.

[8] Arndt, R.E.A., Fuchs, H.V., and Michel, U., "Laboratory Study of Jet Noise Suppressors," *Journal of Acoustical Society of America*, Vol. 63, April 1978, pp. 1060-1068.

[9] Chan, Y.Y. and Templin, J.T., "Suppression of Spatial Waves by Distortion of Jet Velocity Profile," *The Physics of Fluids*, Vol. 17, Nov. 1974, pp. 2124-2125.

[10] Ffowcs Williams, J.E. and Kempton, A.J., "The Noise from the Large-Scale Structure of a Jet," *Journal of Fluid Mechanics*, Vol. 84, Part 4, 1978, pp. 673-694.

[11] Loeffler, I.J., "QCSEE Engine and Wing Tests at NASA," NASA Conference Publication 2077, 1979, pp. 249-261.

[12] Blake, W.K., "A Statistical Description of Pressure and Velocity Field at the Trailing Edges of a Flat Strut," David W. Taylor Naval Ship Research and Development Center, Bethesda, Md., Rept. 4241, Dec. 1975.

[13] Crouch, R.W., Coughlin, C.L., and Paynter, G.C., "Nozzle Exit Flow Profile Shaping for Jet Noise Reduction," AIAA Paper 76-511 presented at the AIAA 3rd Aeroacoustics Conference, Palo Alto, Calif., July 1976.

[14] Brown, W.H., Searle, N., Blakney, D.F., Pennock, A.P., and Gibson, J.S., "Noise Characteristics of Upper Surface Blown Configurations: Experimental Programs and Results," NASA CR-145143, Oct. 1977.

[15] Becker, R.S. and Maus, J.R., "Acoustic Source Location in the Secondary Mixing Region of a Jet-Blown Flap Using a Cross-Correlation Technique," AIAA Paper 77-1364 presented at the AIAA 4th Aeroacoustics Conference, Atlanta, Ga., 1977.

[16] Mani, R., Clapper, W.S., Stringas, E.J., and Banerian, G., "Development of a Technique for In-Flight Jet Noise Simulation—Part II," *Journal of Aircraft*, Vol. 15, Sept. 1978, pp. 589-596.